Atmos. Meas. Tech. Discuss., 8, 13377–13421, 2015
www.atmos-meas-tech-discuss.net/8/13377/2015/
doi:10.5194/amtd-8-13377-2015

Atmospheric Measurement Techniques Discussions
Open Access

Organic and inorganic decomposition products from the thermal desorption of atmospheric particles

B. J. Williams[1], Y. Zhang[1], X. Zuo[1], R. E. Martinez[1], M. J. Walker[1], N. M. Kreisberg[2], A. H. Goldstein[3], K. S. Docherty[4,5], and J. L. Jimenez[5]

[1]Dept. of Energy, Environmental & Chemical Engineering, Washington University in St. Louis, St. Louis, MO, USA
[2]Aerosol Dynamics Inc., Berkeley, CA, USA
[3]Dept. of Environmental Science, Policy & Management and Dept. of Civil & Environmental Engineering, University of California, Berkeley, CA, USA
[4]Alion Science and Technology, EPA Office of Research and Development, Research Triangle Park, NC, USA
[5]Cooperative Institute for Research in the Environmental Sciences (CIRES) and Dept. of Chemistry & Biochemistry, University of Colorado, Boulder, CO, USA

Received: 23 November 2015 – Accepted: 10 December 2015 – Published: 18 December 2015

Correspondence to: B. J. Williams (brentw@wustl.edu)

Published by Copernicus Publications on behalf of the European Geosciences Union.

Abstract

Atmospheric aerosol composition is often analyzed using thermal desorption techniques to evaporate samples and deliver organic or inorganic molecules to various designs of detectors for identification and quantification. The organic aerosol (OA) fraction is composed of thousands of individual compounds, some with nitrogen- and sulfur-containing functionality, and often contains oligomeric material, much of which may be susceptible to decomposition upon heating. Here we analyze thermal decomposition products as measured by a thermal desorption aerosol gas chromatograph (TAG) capable of separating thermal decomposition products from thermally stable molecules. The TAG impacts particles onto a collection and thermal desorption (CTD) cell, and upon completion of sample collection, heats and transfers the sample in a helium flow up to 310 °C. Desorbed molecules are refocused at the head of a GC column that is held at 45 °C and any volatile decomposition products pass directly through the column and into an electron impact quadrupole mass spectrometer (MS). Analysis of the sample introduction (thermal decomposition) period reveals contributions of NO$^+$ (m/z 30), NO$_2^+$(m/z 46), SO$^+$ (m/z 48), and SO$_2^+$(m/z 64), derived from either inorganic or organic particle-phase nitrate and sulfate. CO$_2^+$ (m/z 44) makes up a major component of the decomposition signal, along with smaller contributions from other organic components that vary with the type of aerosol contributing to the signal (e.g., m/z 53, 82 observed here for isoprene-derived secondary OA). All of these ions are important for ambient aerosol analyzed with the aerosol mass spectrometer (AMS), suggesting similarity of the thermal desorption processes in both instruments. Ambient observations of these decomposition products compared to organic, nitrate, and sulfate mass concentrations measured by an AMS reveal good correlation, with improved correlations for OA when compared to the AMS oxygenated OA (OOA) component. TAG signal found in the traditional compound elution time period reveals higher correlations with AMS hydrocarbon-like OA (HOA) combined with the fraction of OOA that is less oxygenated. Potential to quantify nitrate and sulfate aerosol mass concentrations using the TAG system is explored through analysis of ammonium sulfate and ammonium nitrate standards. While chemical standards display a linear response in the TAG system, re-desorptions of the CTD cell following ambient sample analysis shows some signal carryover on sulfate and organics, and new desorption methods should be developed to improve throughput. Future standards should be composed of complex organic/inorganic mixtures, similar to what is found in the atmosphere, and perhaps will more accurately account for any aerosol mixture effects on compositional quantification.

1 Introduction

Atmospheric aerosols have detrimental impacts on human health (Mauderly and Chow, 2008; Pope and Dockery, 2006; Schlesinger et al., 2006) and direct and indirect effects on the global forcing of climate (Carslaw et al., 2013; Heald et al., 2014; Wang et al., 2013). The extent of health and climate impacts is largely dependent on aerosol composition. Fine-mode atmospheric particles are composed of a mixture of inorganic species (e.g., sulfate, nitrate, ammonium), a complex mixture of organic molecules and oligomers, and smaller mass contributions from elemental carbon and metals (e.g., Kim et al., 2005). Fine-mode particulate matter is derived from a range of primary sources, such as combustion, and secondary sources where gases oxidize in the atmosphere to produce lower volatility products that create secondary aerosol. Globally, the majority of fine PM is secondary in nature and made up of thousands of individual chemicals (Jimenez et al., 2009; Ng et al., 2010; Goldstein and Galbally 2007), creating challenges in apportioning the original emission sources of this material, formation pathways, and oxidative evolution in the atmosphere.

The atmospheric formation of secondary inorganic material is relatively well understood. Gas-phase ammonia, nitrogen oxides, and sulfur oxides undergo atmospheric transformations to form stable particle-phase ammonium nitrate and ammonium sulfate. There are various ways to quantify the inorganic composition of atmospheric

Title Page
Abstract | Introduction
Conclusions | References
Tables | Figures
◀◀ | ▶▶
◀ | ▶
Back | Close
Full Screen / Esc
Printer-friendly Version
Interactive Discussion

aerosol. Offline analysis of inorganic ions has been widely utilized (Chow et al., 2008; Nejedlý et al., 1998; Yu et al., 2005), as well as online analysis through direct thermal desorption techniques (e.g., AMS, Canagaratna et al., 2007; ACSM, Ng et al., 2011), ion chromatography (e.g., Weber et al., 2001), and other particle nitrate and sulfate monitors (Drewnick et al., 2003; Stolzenburg and Hering, 2000; Weber, 2003). Organic composition can be determined by a number of offline techniques (e.g., Dillner and Takahama, 2015; Duarte et al., 2015; Finessi et al., 2012; Gaffney et al., 2015; Graham, 2002; Yu et al., 2011) as well as online techniques (e.g., Lanz et al., 2007; Williams et al., 2007). Many online and offline techniques have been summarized previously (Hallquist et al., 2009; Nozière et al., 2015), and each of these methods has strengths and weaknesses when determining the chemical composition of atmospheric aerosol.

The AMS offers online analysis of major inorganic species as well as total organic aerosol (OA) mass concentrations. Additionally, the high resolution time-of-flight AMS can provide elemental composition (e.g., O, C, H, N). Elemental ratios of O : C and H : C can be utilized to estimate the average carbon oxidation state ($\mathrm{OSc} \sim 2 \times (\mathrm{O:C}) - (\mathrm{H:C})$) (Kroll et al., 2011) of ambient OA. Through factor analysis techniques (e.g., positive matrix factorization (PMF), Ulbrich et al., 2009), major OA components can be determined from measured AMS mass spectra, which can be used to infer major source types or atmospheric processes contributing to ambient OA.

The AMS however does not measure individual organic molecules and is thus limited in informing on exact source types. The TAG instrument is an automated in-situ instrument to determine hourly concentrations of hundreds of major contributing organic compounds (Williams et al., 2006, 2010). TAG utilizes a collection and thermal desorption (CTD) cell to collect and thermally transfer samples in helium gas to a GC column. Compounds eluting from the GC at different retention times are then detected by quadrupole mass spectrometry, and more recently by high resolution time-of-flight mass spectrometry in a combined TAG-AMS instrument (Williams et al., 2014). The same factor analysis techniques (e.g., PMF) can be used with TAG data to determine the molecular composition of major contributing components, offering more specific information to infer source types or aerosol transformation processes (Williams et al., 2010). The CTD based TAG system without online derivitization has limited mass transfer of highly oxygenated OA. While this issue has been addressed to some degree in the Semi-Volatile TAG (SV-TAG) system with online derivitization (Isaacman et al., 2014; Zhao et al., 2013), it is of interest to know what fraction of the total OA mass loading is detected by the TAG system. This important question is currently undergoing a detailed investigation and is the focus of a future manuscript, however for the purposes of this work focused on aerosol thermal decomposition, we provide a brief description of what is currently understood regarding mass transfer through the CTD based TAG system as deployed in multiple field campaigns (e.g., Williams et al., 2007, 2010; Kreisberg et al., 2009; Lambe et al., 2009; 2010; Worton et al., 2011).

It has been previously documented that the TAG system detects around 20 % of the total OA (Williams et al., 2006), however it is important to clarify that this fraction is an estimated average. The fraction of total OA seen by the in-situ TAG system is dependent on the type of aerosol being analyzed. If the aerosol is purely composed of hydrocarbons, typically seen in primary OA (POA), the TAG system can potentially thermally desorb, transfer, and detect up to 100 % of the total POA mass based on what is observed through analysis of calibration standards and high correlations between TAG POA components and AMS hydrocarbon-like OA (HOA) components in ambient aerosol (Williams et al. 2010; Zhang et al., 2014). The more oxidized the aerosol becomes, whether through photochemically produced secondary OA (SOA) or aging of POA, the TAG system will detect a smaller fraction of the total OA mass. We have observed through mass transfer tests that a fraction of the oxidized material does not transfer through a typical 30 m GC column. Additionally, we have now observed (described here) that a fraction of the oxygenated aerosol thermally decomposes during initial heating and transfer to the GC column from the CTD cell. Previously, the MS detector was turned off during this desorption period to protect from high signals that may come from water vapor or solvent used during calibration standard injections. This "solvent delay" is common GC practice. We no longer use a solvent delay since we have observed decomposition products during this period, and their measurement can potentially provide useful information about aerosol composition. Analysis of these decomposition products is the focus of this paper.

Thermal decomposition has been observed in many previous technologies (Canagaratna et al., 2007; Chow et al., 2007), and is often utilized as the operating principle for many of these techniques. Often, thermal desorption for such methods occurs at higher temperatures (up to 500–900 °C) than achieved in the TAG system that reaches a maximum temperature of 310 °C which is limited by the maximum temperature of the GC columns used and thus the range of chemicals expected to elute through the column. Additionally, in other methods there is often intentional catalytic conversion of a range of decomposition products to easily-measurable gas-phase species (e.g., CO_2 for organics, SO_2 for sulfate, NO for nitrate) that can be detected and quantified by simple gas monitors. It is also important to note that thermal desorption in the TAG system occurs in a dominantly helium environment with trace quantities of N_2 and O_2 present that cannot be fully purged, although approximately 40 volume flushes are performed with ultra high purity helium prior to heating. With the lower temperatures and dominantly inert environment found in the TAG CTD cell and transfer line, it is uncertain how thermal decomposition from the TAG system compares to other techniques. Here we investigate for the first time the thermal decomposition products observed by the TAG system and provide new insight on how these products can be better utilized in future studies to inform on the organic and inorganic composition of ambient aerosol. It is also worth noting that TAG CTD cells are now used as the collection and sample introduction system for a range of instruments including a proton transfer reaction mass spectrometer (PTRMS, Holzinger et al., 2010), Semi-Volatile TAG (SV-TAG, Zhao et al., 2013) which utilizes a metal fiber filter collector in place of the inertial impactor, two dimensional TAG (2D-TAG, Goldstein et al., 2008), and a volatility and polarity separator (VAPS, Martinez et al., 2015), and thermal decomposition analysis explored here could also be applied to these technique variants.

2 Aerosol components observed by TAG

Details of TAG design, calibration, and operation can be found in previous manuscripts (Kreisberg et al., 2009; Williams et al., 2006, 2007, 2010). A brief overview is offered here. The TAG system collects ambient aerosol through cyclone precut (most often PM_1 or $PM_{2.5}$) to determine an upper size limit, and is humidified to increase particle adhesion upon inertial impaction in the CTD cell. After sufficient sample is collected (typically 30 min collection at 9 L min^{-1}), the sampling system switches to a bypass mode and the CTD cell is purged for 5 min with helium at 50 °C (see Fig. 1 for an example sample). Some purging of the most volatile fraction is required in order to eliminate some water vapor from ambient sampling or solvent from calibration standard injection. Thermal denuder AMS studies have observed evaporation of nitrate aerosol (up to 20 %), OA (up to 10 %), and sulfate (few percent) at 50 °C (Huffman et al., 2009), and a $PM_{2.5}$ tapered element oscillating microbalance (TEOM) mass monitor operated with a sample stream at 50 °C has shown a 14 % decrease (on average) in aerosol mass compared to a 30 °C sample stream (Meyer et al., 2000). A minor fraction of these components will be lost during the purge time period. Following the volatile-component purge period, the CTD cell is switched to thermally inject sample onto the GC column which is held at a cooler 45 °C, while the CTD cell temperature ramps from 50 °C up to 310 °C over approximately 4 min and is held at 310 °C for an additional 6 min. Next, the CTD cell injection valve is switched back to a "load" position and cooled to prepare for the next sample collection. Meanwhile, the previous sample is recondensed at the start of the 30 m GC column (TAG traditionally uses a low-polarity column, e.g., 5 % diphenyl/95 % dimethyl polysiloxane) and is then slowly thermally ramped (10 °C min^{-1}) to 310 °C and held at maximum temperature for 10 min. During this time period, resolved compounds and unresolved complex mixtures elute from the GC column and are detected by electron impaction ionization (70 eV) quadrupole mass spectrometry (QMS). We have previously operated the QMS in a scan range of m/z 29–550. The lower limit of m/z 29 was established to eliminate large signals associated with H_2O

(m/z 18) and N_2 (m/z 28) to prolong detector lifetime, but still includes O_2 (m/z 32) and Ar (m/z 40) to allow detection of any leaks that could be developing in the CTD cell or GC column. Upon completion of the GC/MS analysis, the GC oven is cooled in preparation for the next sample injection that has been collected on the CTD cell during the GC/MS analysis of the previous sample.

Figure 1 shows an example of this process as observed on the QMS (showing total ion count, summed ions in the established range of m/z 29–550). We now operate the QMS detector to acquire data during the entire cycle, as opposed to previous operation that incorporated a solvent delay of approximately 15 min that eliminated the large signal during delivery from the CTD cell onto the column. Shown here is an ambient sample (in black) compared to a CTD cell blank (in gray) that is simply a re-desorption of the previous sample without further sample collection. In looking at the cell blank, it can be seen that there is some signal associated with the sample injection/thermal decomposition window (defined as the time window between 6–16 min, which is 5–15 min plus a ∼ 1 min delay in transferring even the most volatile species through a 30 m GC column). The terms thermal desorption period, sample injection period, and thermal decomposition window will be used interchangeably based on which process is being discussed. The cell blank material present in this analysis window is largely attributed to small amounts of oxygen present in the cell (m/z 32) and degradation of the graphite/vespel ferrule material used on the CTD cell (this ferrule material has been chosen for ease of replacement since they are not permanently attached to components). After the occasional replacement of these ferrules, the CO_2 (m/z 44) signal within the sample injection period increases, then decreases over a number of thermal cycles to a stable signal. The cell blank also has significant signal in the time window of 40–55 min due to what is known as column bleed. The stationary phase of the GC column is always slowly eluting through the column, resulting over a long period of time in the need for column replacement due to insufficient phase interaction with analytes. Column bleed is observed in all cell blanks as well as ambient samples.

The ambient sample (in black) has an elevated signal in the thermal decomposition window (which will be the focus of this paper) for some ions with $m/z < 100$ (Fig. 1b), as well as during the GC column temperature ramp and hold (16–45 min), which has been the focus of previous TAG papers. Previous papers have not discussed the thermal decomposition window, but here we demonstrate the additional and complementary information it contains. The sharp peaks are resolved compounds that can be identified based on their retention times and their characteristic mass spectral fragment patterns and matched to mass spectral databases (e.g., NIST mass spectral database). There is additional material found between these resolved peaks and the baseline set by the cell blank. This material is often referred to as an unresolved complex mixture (UCM) in GC terms and is composed of hundreds of overlapping species that typically have common mass spectral structure (i.e., many isomers of similar compounds and classes), making them difficult to distinguish from one another. Recent advances have been made to further resolve the UCM signal (e.g., 2D-GC, Goldstein et al., 2008) and to bin chromatograms to fully incorporate UCM signal within OA composition analyses (Zhang et al., 2014).

To further investigate the TAG thermal decomposition window (6–16 min) we examine specific ion signals (Fig. 1) and demonstrate they provide useful markers for organic as well as inorganic aerosol. To update from previous literature (Williams et al., 2014) on the fractions of total fine aerosol as observed by TAG, it is now understood that the TAG fractions include: (1) resolved compounds (RC), (2) unresolved complex mixture (UCM), (3) non-eluting organics (NEO) composed of highly oxygenated organics that do not transfer through a long 30 m GC column, (4) purged semivolatile organics (PSO) that were purged at the start of the analysis cycle, (5) thermally decomposed organics (TDO) composed of organic species that experience thermal decomposition upon heating, thought to be highly oxygenated molecules, oligomeric material, or inorganic species formed from decomposition of organic species (e.g., organonitrates which are known to be thermally labile), (6) thermally decomposed inorganics (TDI) such as nitrate and sulfate decomposition fragments observed in the thermal decomposition window, (7) purged semivolatile inorganics (PSI) that were purged at the start of the analysis cycle, and (8) non-eluting inorganics (NEI) composed of any remaining aerosol fractions not detected on the TAG system (e.g., metals, metal oxides, other crustal elements, elemental carbon, and potentially sea salt if HCl from NaCl decomposition is not detected). Therefore, the total aerosol classified according to these TAG fractions can be summed as:

$$\begin{aligned}\text{Total Aerosol} &= \text{Organics (RC + UCM + PSO + NEO + TDO)}\\ &\quad + \text{Inorganics (TDI + PSI + NEI)}\end{aligned}$$

Further characterization and quantification of these fractions for various laboratory and ambient aerosol types is of high priority.

3 Thermal decomposition products observed by TAG

Thermal decomposition products were first observed in TAG data when reviewing a previous data set from the Study of Organic Aerosols at Riverside (SOAR-1) that took place in Riverside, CA during the summer of 2005. Here, the TAG QMS detector was set to have a traditional solvent delay, then would turn on during the final minute of the CTD cell thermal desorption cycle in order to track any air leaks that could develop in the cell during normal field operation (see Fig. S1 in the Supplement). In reviewing the final minute of the thermal desorption cycle, it was observed that besides just O_2 (m/z 32) and Ar (m/z 40), which were used to track air leaks, there were other ions present, including m/z 30, 44, 48, and 64. Integrating these ions over the 1 min elution period and over the course of a previously defined study focus period (Williams et al., 2010) revealed reasonable correlations between TAG m/z 64 and AMS sulfate (Pearson $r = 0.59$), TAG m/z 44 and AMS organics ($r = 0.51$), and a very good correlation between TAG m/z 30 and AMS nitrate ($r = 0.93$) (revisited in further detail below).

During a recent ambient field study, the St. Louis Air Quality Regional Study (SLAQRS) that took place in East St. Louis, IL during the summer and fall of

2013, the TAG system was programmed to acquire QMS data throughout the entire CTD cell thermal desorption period to gain a more complete picture of eluting thermal decomposition products at the expense of regularly exposing the detector to larger signals and potential shorter detector lifetime. Ions below m/z 29 were still excluded to limit detector exposure to large N_2 (m/z 28) and H_2O (m/z 18) signals.

Figure 2 highlights an example TAG sample with significant contributions from various organic and inorganic ions within the decomposition window for an ambient aerosol sample (Fig. 2a) compared to a following cell blank (Fig. 2b). For this cell blank, the sample valves open as usual but the sample flow is shut off to prohibit particle collection, and the cell is then thermally cycled in an identical manner as during an actual sample acquisition. Here it is observed that there is excess signal present in the ambient sample, indicating some highly volatile components are released directly from the collected particles. Considering material that makes it to the detector during this period needs to travel through 30 m of a GC column held at a low temperature of 45 °C, it is very unlikely that this highly volatile material was originally present in the particle phase in this form, but rather it was thermally decomposed from larger molecules or oligomers. It is also noticed in this sample that the cell blank still has a significant amount of material present during the desorption cycle. A large fraction of the signal is from m/z 32 (O_2) as would be expected whether or not particles are collected since it is present largely due to small dead volumes that are not efficiently flushed with helium between samples. Figure S2 in the Supplement highlights that m/z 32 during the sample injection period is dramatically reduced if sample valves remain closed from the previous desorption cycle and new air is not allowed to enter the helium-filled CTD cell.

Figure 3 highlights the full thermal decomposition product window observed by TAG for three different aerosol types observed during the SLAQRS field campaign. Panels a and b show a sample that had a relatively elevated m/z 30 signal, panels c and d show a sample that had relatively elevated m/z 48 and m/z 64, and panels e and f show a sample that had relatively elevated m/z 53 and m/z 82. The top panels of each set (a, c, e) display individual ions of interest, and the bottom panels (b, d, f) show cumulative traces of all major ions. The bottom panels show that these 10 ions alone account for 85–90 % of the total ion signal in the thermal decomposition window for these three aerosol types. All samples show a similar elution pattern for m/z 32 (O_2), increasing immediately as the CTD cell valve is switched to inject the sample onto the GC column, and slowly decays a little over the 10 minute injection. In contrast, the general trend for m/z 44 (CO_2) is to slowly increase with increased temperature and reach a stable value or even slightly decrease at top temperature. This slow increase with increased temperature indicates that the CO_2 is indeed a decomposition product coming from the CTD cell as opposed to CO_2 gas remaining in the cell after 5 min of helium purging, where it would have an immediate increase as seen in the O_2 signal. The signal detected in this thermal decomposition product window is similar to the thermograms produced by other in-situ measurement system like the MOVI (Brüggemann et al., 2014; Yatavelli et al., 2012) and FIGAERO (Lopez-Hilfiker et al., 2014, 2015) inlets for mass spectrometers, or the thermal desorption particle beam mass spectrometer (TDPBMS) (Lim and Ziemann, 2009; Tobias et al., 2000, 2001), which have all obtained information on the thermal stability of organic species. The difference here is that thermally stable species are retained by the TAG GC column and detected later in the compound window, whereas these other techniques first detect the thermally stable components (without molecular separation), then detect the thermal decomposition products at the end of the temperature ramp.

The sample in Fig. 3 panels a and b is taken from a period with elevated aerosol nitrate according to a collocated AMS. Here, m/z 30 and 46 are elevated, indicating they represent NO and NO_2 decomposition fragments, just as observed in the AMS system. Ammonium nitrate and organic nitrates are relatively volatile species and it is expected they would volatilize within the lower temperature limit of the TAG cell (310 °C). The sample in panels c and d, with elevated m/z 48 and 64 correspond to a time period with elevated sulfate, indicating these ions represent SO and SO_2 decomposition fragments. These ions increase later in the decomposition window than the organics or nitrate ions. Both laboratory and field measurements have shown ammonium sulfate to be less volatile than ammonium nitrate (Hering and Cass, 1999; Huffman et al., 2009). Volatilized ammonium nitrate and ammonium sulfate would produce gas phase ammonia (m/z 17, which is below our QMS scanning range) and gas phase nitric acid (m/z 63) or sulfuric acid (m/z 98). In order of relative abundance, the EI mass spectrum for sulfuric acid is composed of the fragments m/z 80, 81, 48, 64, 98 (NIST mass spectral database) and for nitric acid the fragments m/z 46, 30 (Friedel et al., 1959). It is unlikely that nitric acid and sulfuric acid are transferred efficiently through the TAG collection cell, through the 30 m GC column, and into the QMS detector. It is more likely that the major ions observed here (NO^+, NO_2^+, SO^+, SO_2^+) result from stable species (e.g. NO, NO_2, SO, SO_2) created in the CTD cell. This could either result purely from the elevated temperature (maximum of 310 °C), or perhaps the catalytic conversion of nitric or sulfuric acid by the CTD cell walls where there could be stainless steel exposed, or perhaps with the Inertium surface coating (proprietary coating from AMCX Inc. used on the CTD cell walls and all transfer lines to the GC column). While the exact mechanism remains unclear, such catalytic conversion has been utilized in previously developed measurement techniques (Drewnick et al., 2003; Yamamoto and Kosaka, 1994).

The AMS community has established a ratio of the ions m/z 46/30 to determine a difference between inorganic nitrate and organic nitrate (e.g., Fry et al., 2013), with organic nitrates displaying an elevated m/z 30 signal. With the TAG system, a majority of the nitrate signal always appears at m/z 30, with a change in the m/z 46/30 ratio observed with nitrate mass loading. It is unclear if this ratio will be informative of differences between inorganic and organic nitrate, but perhaps future comparisons of m/z 30 and 46 elution times in the decomposition window, using known standards, will offer insight on differing origins of the nitrate material.

The sample in Fig. 3 panels e and f is taken from a period with elevated OA according to the AMS and arrives to the site from the southwest. Additionally, gas-phase measurements of isoprene and its oxidation products methacrolein and methyl vinyl ketone are elevated with these southwesterly air masses transecting the Ozark oak forests of southern Missouri. We expect to see isoprene-derived SOA in these air masses.

Recently, the AMS community has reported a mass spectral marker for low-NOx isoprene-derived SOA that has high m/z 53 and m/z 82 (Hu et al., 2015; Robinson et al., 2011; Slowik et al., 2011). It was first suggested that the elevated signal of m/z 53 and 82 was from methylfuran detected as a thermal decomposition product of isoprene SOA (Robinson et al., 2011). Recently it has been shown that SOA molecules formed form isoprene epoxydiols (IEPOX) that are formed under low-NO_x conditions in the presence of acidic seed particles will form isomers of 3-methyltetrahydrofuran-3,4-diols. Isomers of IEPOX and 3-methyltetrahydrofuran-3,4-diols have been shown to contain ions m/z 53 and 82 when analyzed by thermal desorption, electron impact ionization techniques such as the AMS (Lin et al., 2012). Although IEPOX isomers are too volatile to be present in the particle phase directly, further gas-phase or particle-phase transformations may create IEPOX-derived SOA products that thermally decompose to similar fragments, like is observed in the case of the 3-methyltetrahydrofuran-3,4,-diols. A method to quantify total IEPOX-SOA using a background corrected m/z 82 ion signal has now been established (Hu et al., 2015).

The same ions (m/z 53 and 82) are found to be high during isoprene SOA-influenced time periods during the SLAQRS field study according to ambient TAG data. The majority of the m/z 53 and m/z 82 signal is found within this thermal decomposition window, while there are some additional molecules at lower relative abundance that do appear in the regular GC analysis period (16–50 min) (see Fig. S3). Further study of isoprene-derived SOA thermal decomposition is currently under investigation using reference standards and laboratory generated aerosol.

Beyond expected total signal variability between ambient samples, closer evaluation between samples reveals measurable variation in the rate of increase during desorption which could indicate different decomposition temperatures for various types of organics, nitrates, and sulfates (see example in Fig. S4). Organics appear to also display differences in thermal desorption profiles. It has been observed through thermal denuder measurements (Huffman et al., 2009) with the AMS that OA has different volatilities based on degree of oxidation, and two major classifications of oxygenated OA (OOA) have been established based on their volatility differences: semivolatile-OOA (SV-OOA) and low volatility-OOA (LV-OOA), where LV-OOA typically represents a more oxidized/aged aerosol. Further characterization of the desorption profile for CO_2 observed here may offer similar information on OA type and volatility. Differences in desorption profiles for nitrates and sulfates could represent a difference between organic and inorganic fractions. Further characterization using synthesized standards is required to explore this possibility.

4 Carryover from previous samples

It is observed that each of the decomposition products recorded in the injection period window displays varying degrees of desorption efficiency through a single desorption cycle. Figure 4 highlights this point by comparing consecutive ambient sample, denuded sample, followed by multiple cell blanks where the sample valves open but the sample pump has been disabled, not allowing new sample collection. The m/z 46 (NO_2^+) fragment is much smaller in comparison to m/z 30 (NO^+) and appears to have an elevated background (Fig. 4g), making it a poor tracer for nitrate. Here we see that for the nitrate tracer (m/z 30, Fig. 4c, g), the sulfate tracers (m/z 64 and m/z 48, Fig. 4a, e), the organics tracer (m/z 43, Fig. 4f), and the isoprene-derived SOA tracers (m/z 53 and m/z 82, Fig. 4d, h), the ambient sample and denuded ambient sample have very similar signal, indicating they are almost entirely present in the particle-phase. The tracers m/z 44 and m/z 46 display a higher background signal compared to other tracer ions, even after several repeat blanks.

Ammonium nitrate is known to be more volatile compared to ammonium sulfate (Huffman et al., 2009). The sulfate tracers (m/z 64 and 48, Fig. 4a, e) do not appear to fully volatilize/fragment on a single desorption cycle. Here it is seen that while the first cell blank has dramatically reduced signal, subsequent cell blanks show continued volatization/decomposition of sample remaining from previous sample collection. The organic tracers (m/z 44 and 43, Fig. 4b, f) also show that continued re-desorptions of the denuded sample produces additional m/z 44 and 43 signal above background. Here it is better observed that the remaining background of m/z 44 signal is elevated due to the effect of degradation of ferrules as discussed previously. Replacing as many ferrules with metal ferrules where possible will help to lower the m/z 44 background signal in future studies. Carryover of m/z 43, 44, 48, and 64 could result in a slight smoothing-type effect when tracking abundance changes over time or a tailing effect following large spikes in concentration. Modifications to the thermal desorption profile can be explored to help minimize carryover. The maximum temperature limit remains due to material constraints, however longer holding times at maximum temperature could be implemented.

5 Calibration

Since the TAG system has never been applied for monitoring inorganic aerosol fractions, it is of interest to determine whether the signal present in the decomposition window is in any way a quantitative measure of the amount of inorganic aerosol present in ambient samples. To explore this question, known quantities of ammonium nitrate and ammonium sulfate solutions were injected into the TAG CTD cell. Major decomposition ions m/z 30 and m/z 64 were integrated across the decomposition window (6–16 min) and are plotted with injected mass in Fig. 5. A linear response is observed for both inorganic species. Ammonium is not quantified due to the mass scan range of the QMS as described earlier. According to these injections of pure inorganic composition, the limit of detection for ammonium sulfate is not approached at the smallest injection of 350 ng and is in the range of 400 ng for ammonium nitrate (when extrapolating from the smallest injection quantity). Since the TAG system conventionally acquires approximately 0.26 $\mathrm{m^3}$ sample volume per sample, these detection limits would require that at least 1.24 $\mu\mathrm{g\,m^{-3}}$ of nitrate (1.6 $\mu\mathrm{g\,m^{-3}}$ in the form of ammonium nitrate) be present in the ambient aerosol for detection by TAG. It is observed in ambient measurements that TAG is likely able to detect much lower concentrations of nitrate when sampled in a complex mixture that contains organics and inorganics as will be shown below (e.g., good correlations observed with nitrate concentrations below $0.5\,\mu\mathrm{g\,m^{-3}}$ in the field), and our extrapolated estimate for ammonium nitrate limit of detection is likely overestimated. Additionally, the pure ammonium sulfate standard appeared to cause damage to the surface coating of the CTD collection cell and GC column when injected as a pure component, perhaps through the production of sulfuric acid. However, months-worth of use in the field where sulfate is present within a complex aerosol mixture does not appear to cause significant surface damage.

Both of these observations (i.e., better detection of nitrate in a mixture and surface coating damage from pure ammonium sulfate) suggest the need for a calibration standard that is a complex mixture of organic and inorganic components when extending TAG analyses to include the inorganic fraction. This is consistent with AMS experience where complex ambient particles are detected better than pure particles (Middlebrook et al., 2012), and matrix effects have been reported in previous TAG work, where detection of certain organic molecules was increased with higher loading of ambient black carbon mass in field observations and with higher loading of a co-injected motor oil in lab studies (Lambe et al., 2010). The TAG already uses a wide range of nonpolar and single-functionality polar molecules for calibrating resolved organic compounds. Once the nature of the m/z 44 signal (and other contributing organic ions) within the decomposition window are better understood, additional appropriate organic calibration components can be added to the calibration standard mixture, for example citric acid and oxalic acid have been shown to undergo significant decomposition with thermal desorption (Canagaratna et al., 2015).

6 Correlation with AMS Species

It is of interest to determine how these decomposition products behave in ambient field samples collected over a period of time with variable source contributions. Here, we again use ambient field data collected on TAG during the SLAQRS field campaign in East St. Louis, IL. TAG measurements occurred in three distinct sampling cycles. The first and last study period rotated between ambient samples (where the CTD cell collects particles + adsorbing semivolatile gases) and filtered ambient samples (where the CTD cell collects adsorbing semivolatile gases only) using Teflon filters upstream of the collection cell to remove the particle fraction. Filtered data has been interpolated onto the ambient data timeline and subtracted from ambient data to derive a particle-only time series. The mid study period rotated between ambient and denuded ambient (particle only) data. The denuded ambient data represents the particle-only time series for this study period. Since there is no subtraction of background (cell blank) signal when using denuded data, additional subtraction is accounted for by acquiring regular cell blanks, interpolating cell blanks onto denuded time line, determining an average percentage of cell blank signal compared to denuded sample signal, and finally subtracting this fraction from each denuded sample. Figure S5 displays the resulting time series for background-subtracted particle-only signal for m/z 30, 44, 53, 64 respectively. The values shown for TAG fragments are integrated single ion signals on the QMS across the entire 6–16 min decomposition window.

The oxygen content present in the decomposition period can drift over the course of a multi-week study. It is worth considering whether the amount of oxygen present has an effect on the amount of organic or inorganic decomposition product as observed by the TAG system. There would be a likely dependence if the trace oxygen content was in some part responsible for any of the observed volatile fragments, e.g. from oxidation of "charred" material. In tracking the correlation of the major observed fragments present in the decomposition window with oxygen in the decomposition period, there is no observed evidence for decomposition fragment signal on oxygen content ($r = -0.13$, -0.11, -0.02, -0.32 for particle-only m/z 64, 44, 30, 53, see Fig. S6).

A high resolution time-of-flight AMS (HR-ToF-AMS; DeCarlo et al., 2006) was also deployed on the SLAQRS study and measured ambient mass concentrations of fine mode (PM_1: particulate matter with aerodynamic diameter < 1 µm) aerosol nitrate, sulfate, and total organics. The TAG inlet also utilized a PM_1 cyclone to match the particle size collection of the AMS system. Figure 6 shows overlapping time lines of AMS species and TAG fragments present in the decomposition window. Figure panels a–d highlight reasonable correlation between TAG fragments and AMS species timeseries. Figure panels e–h highlight the observed correlation is only observed with appropriate adjustments to determine a particle-only fraction (e.g., filter subtractions during the early and late study period and blank subtractions from denuded samples in the mid study time). The observed slopes could be used as empirical calibrations of the TAG fragments to convert relative abundance signal to mass concentrations. In the absence of co-located AMS data, appropriate calibration standards as mentioned previously would need to be regularly injected. Exceptions are TAG decomposition fragment m/z 46 (Fig. 6e) which does not have a good correlation with AMS nitrate, and TAG decomposition fragment m/z 82 (Fig. 6h) which does not have a good correlation with AMS m/z 82. It has already been discussed that the TAG decomposition fragment m/z 46 (NO_2^+) has very little signal, and it has been previously shown that AMS m/z 82 has contributions from other non-isoprene sources (Hu et al., 2015) which may be present in the TAG compound window and not included in this decomposition signal (see Fig. S3).

The correlation between AMS organics and particle-only TAG m/z 44 within the decomposition window is improved when only the oxygenated component of the AMS organics signal is included. AMS data can be fit to a 2-factor PMF solution to yield a hydrocarbon-like OA (HOA) that is often more primary in origin and an oxygenated OA (OOA) component that is often more secondary in origin (believed to be formed primarily from gas-to-particle photochemical conversion in the atmosphere). The TAG decomposition m/z 44 time series has a correlation with AMS OOA ($r = 0.58$) that is higher than the observed correlation with AMS total OA ($r = 0.46$) or AMS HOA ($r = -0.08$) (see Fig. 7 and Table 1). However, TAG m/z 44 within the decomposition window does not show an improved correlation when comparing it directly to AMS m/z 44 ($r = 0.41$) or AMS CO_2^+ ($r = 0.35$) during the SLAQRS field study (see Table 1). In looking back at the data from the earlier SOAR study, although the entire decomposition window was not recorded, the m/z 44 signal from the final minute of the TAG decomposition window had a correlation with AMS OOA ($r = 0.55$) that was higher than the correlation with AMS total OA ($r = 0.51$) or AMS HOA ($r = 0.02$) (see Table 1). During the SOAR study, the TAG m/z 44 decomposition signal did show an increased correlation with AMS m/z 44 ($r = 0.70$) and AMS CO_2^+ ($r = 0.70$). The TAG m/z 43 signal in the decomposition window, while much lower in signal than m/z 44, also shows improved correlation with AMS OOA compared to just total OA for both studies. TAG m/z 43 decomposition signal has a higher correlation to AMS m/z 43 and AMS $C_2H_3O^+$ for the SLAQRS study compared to the SOAR study (see Table 1). Further controlled lab studies are underway to better characterize these TAG and AMS relationships using known aerosol types across various extents of oxidation.

The AMS PMF solution for the SOAR study was further separated into additional components based on extent of oxidation and volatility (Docherty et al., 2011). Multiple low volatility–OOA (LV-OOA) components were observed and combined into a single source type called cLV-OOA, which accounted for 31.3 % of total observed OA and whose mass spectrum contained a dominant contribution from CO_2^+. This aerosol type is thought to be the most oxygenated and aged aerosol component and has been observed in many studies (Jimenez et al., 2009; Ng et al., 2010). Here, we observe an increased correlation between TAG decomposition m/z 44 signal and cLV-OOA ($r = 0.73$), and an even higher correlation with one of the individual LV-OOA components ($r = 0.90$) (see Table 1), although there is no known explanation in the source or process differentiation between the multiple LV-OOA components. A recent report from Canagaratna et al. (2015) suggests that m/z 44 (CO_2^+) as observed by the AMS is largely from decarboxylation of organic acids.

Both studies (SOAR and SLAQRS) strongly indicate that the m/z 43 and 44 decomposition component measured on the TAG system is from oxygenated OA as opposed to primary hydrocarbon components. Many hydrocarbons are more thermally stable than oxygenated functional groups, and they transfer through the GC column more efficiently than oxygenated molecules. It is thought that most of the HOA material is detected on TAG within the regular chromatogram window (as resolved compounds and UCM). TAG PMF components that contain dominantly hydrocarbons have been shown to correlate well with AMS HOA component in previous studies (Williams et al., 2010; Zhang et al., 2014). Here, we have integrated the total ion signal within the main chromatogram window (16–45 min) and subtracted off the GC column bleed component using a novel method described by Zhang et al. (2014), as well as the gas-phase fraction and remaining background signal (using the same subtraction methods applied to the decomposition window subtractions) to create a particle-only TAG main chromatogram signal time series. For the East St. Louis SLAQRS study, the TAG main chromatogram showed a higher correlation with AMS HOA ($r = 0.60$) than compared to AMS OOA ($r = 0.32$) (see Table 1). The same is true for the Riverside SOAR study, where the TAG main chromatogram had a higher correlation with AMS HOA ($r = 0.60$) compared to with AMS OOA ($r = 0.36$) (see Table 1). An even higher correlation was observed between the particle-only TAG main chromatogram signal and a combination of the higher factor AMS PMF solution components HOA + medium-volatility (MV)-OOA ($r = 0.76$) (see Table 1), indicating that some of the less oxygenated OOA material does transfer through the GC column and contributes to the resolved compounds and UCM components observed in the TAG main chromatogram. TAG PMF components can be derived using resolved compounds (Williams et al., 2010), or with a new binning technique to incorporate the UCM (Zhang et al., 2014). Resulting TAG PMF components that contain less oxygenated (e.g., single oxygenated functionality) semivolatile compounds also correlate with the AMS semivolatile OOA (SV-OOA) and medium-volatility

OOA (MV-OOA) components (Williams et al., 2010; Zhang et al., 2014). However, few resolved compounds show any correlation with the most oxygenated and lowest volatility AMS component (LV-OOA). LV-OOA is dominated by CO_2^+ m/z 44 on the AMS, and we propose that this is what is observed as m/z 44 in the decomposition window of the TAG system.

While good correlation is observed for sulfate between the two instruments, particulate nitrate had a lower correlation and was relatively low in mass concentrations during the overlapping TAG and AMS study periods during SLAQRS (Fig. 6). In comparing the correlation between TAG m/z 30 from the final minute of the previous study in southern California (SOAR) and AMS nitrate, a much higher correlation is observed ($r = 0.93$) (see Fig. 8). Perhaps the higher correlation during SOAR was due to a higher nitrate mass concentration on average (5.6 $\mu g\,m^{-3}$) compared to the overlapping operation period during SLAQRS (0.32 $\mu g\,m^{-3}$), values that were thought to be below detection for this TAG method (according to a pure single-component standard calibration). Inorganic calibration standards were not applied on the TAG system in the field during either study. As shown previously, laboratory calibrations were performed for ammonium sulfate and ammonium nitrate immediately following the SLAQRS study. The mass spectrometer had been retuned and collection system components had been replaced between the field measurements and laboratory tests, so a direct comparison is not possible. However, the lab calibrations have been applied to the field measurements (see Fig. S7) for a general comparison. Here it is observed that the there is a baseline offset of approximately 1.3 $\mu g\,m^{-3}$ and a slope offset of a factor of 0.4 between TAG and AMS nitrate calibration. For sulfate there is a baseline offset of approximately 2.8 $\mu g\,m^{-3}$ and a slope difference of a factor of 3. In addition to retuning, discrepancies could also be due to simple inorganic standards not accurately representing the response to nitrate and sulfate in a complex ambient aerosol matrix. Again, it is recommended that future field studies incorporate a complex calibration standard mixture of inorganics and organics.

Title Page
Abstract Introduction
Conclusions References
Tables Figures
◀◀ ▶▶
◀ ▶
Back Close
Full Screen / Esc
Printer-friendly Version
Interactive Discussion

7 Conclusions and discussion

Since its creation, the TAG system has been utilized for acquiring hourly-resolved time series of organic marker compounds that can be used in factor analyses to determine major contributing sources or atmospheric transformation processes of ambient OA. Here, for the first time, it has been shown that major inorganic aerosol components (i.e., nitrate and sulfate) as well as thermally labile fractions of the OA component will thermally decompose in the TAG collection cell upon heating and transferring material from the collection site to the GC column. These decomposition fragments are volatile and transfer directly through the GC column. By acquiring mass spectral information during this analysis time period, these decomposition fragment ions can be recorded and used to estimate particulate nitrate, sulfate, some fraction of oxygenated OA (likely the most oxygenated fraction), and potentially other OA components (e.g., clear tracers for isoprene-derived SOA were observed here). We have observed good correlations between these TAG thermal decomposition components and the corresponding quantified AMS species.

Quantification of TAG decomposition signals provides an opportunity for future development. While calibration standards display linearity in response, it is proposed that a complex mixture of inorganics, hydrocarbons, and oxygenated organic molecules (including some thermally labile multi-functional species) be utilized for calibration to best mimic an ambient sample. Initial results suggest such a standard would be necessary to improve detection limits and limit the potential for interior surface coating damage to the TAG system caused by acidic vapors. Further use and careful analysis of the mass spectral information contained within the TAG decomposition analysis window and the main chromatogram window will offer new insights on the chemical composition of complex environmental samples.

The Supplement related to this article is available online at doi:10.5194/amtd-8-13377-2015-supplement.

Acknowledgements. This research has been supported by a grant from the U.S. Environmental Protection Agency's Science to Achieve Results (STAR) program. Although the research described in the article has been funded wholly or in part by the U.S. Environmental Protection Agency's STAR program through grant (R835402), it has not been subjected to any EPA review and therefore does not necessarily reflect the views of the Agency, and no official endorsement should be inferred. TAG measurements during SOAR 2005 were supported by the California Air Resources Board (CARB) award number 03-324. KSD and JLJ acknowledge support from NSF (AGS-1243354), DOE (BER/ASR Program, DE-SC0011105) and NOAA (NA13OAR4310063).

References

Brüggemann, M., Lucas Vogel, A., and Hoffmann, T.: Analysis of organic aerosols using a micro-orifice volatilization impactor (MOVI) coupled to an atmospheric-pressure chemical ionization mass spectrometer (APCI-MS), Eur. J. Mass Spectrom., 20, 31–41, doi:10.1255/ejms.1260, 2014.

Canagaratna, M. R., Jayne, J. T., Jimenez, J. L., Allan, J. D., Alfarra, M. R., Zhang, Q., Onasch, T. B., Drewnick, F., Coe, H., Middlebrook, A., Delia, A., Williams, L. R., Trimborn, A. M., Northway, M. J., DeCarlo, P. F., Kolb, C. E., Davidovits, P., and Worsnop, D. R.: Chemical and microphysical characterization of ambient aerosols with the aerodyne aerosol mass spectrometer, Mass Spectrom. Rev., 26, 185–222, doi:10.1002/mas.20115, 2007.

Canagaratna, M. R., Jimenez, J. L., Kroll, J. H., Chen, Q., Kessler, S. H., Massoli, P., Hildebrandt Ruiz, L., Fortner, E., Williams, L. R., Wilson, K. R., Surratt, J. D., Donahue, N. M., Jayne, J. T., and Worsnop, D. R.: Elemental ratio measurements of organic compounds using aerosol mass spectrometry: characterization, improved calibration, and implications, Atmos. Chem. Phys., 15, 253–272, doi:10.5194/acp-15-253-2015, 2015.

Carslaw, K. S., Lee, L. A., Reddington, C. L., Pringle, K. J., Rap, A., Forster, P. M., Mann, G. W., Spracklen, D. V., Woodhouse, M. T., Regayre, L. A., and Pierce, J. R.: Large contribution of natural aerosols to uncertainty in indirect forcing, Nature, 503, 67–71, doi:10.1038/nature12674, 2013.

Chow, J. C., Yu, J. Z., Watson, J. G., Hang Ho, S. S., Bohannan, T. L., Hays, M. D., and Fung, K. K.: The application of thermal methods for determining chemical composition of carbonaceous aerosols: A review, J. Environ. Sci. Health A, 42, 1521–1541, doi:10.1080/10934520701513365, 2007.

Chow, J. C., Doraiswamy, P., Watson, J. G., Chen, L.-W. A., Ho, S. S. H., and Sodeman, D. A.: Advances in Integrated and Continuous Measurements for Particle Mass and Chemical Composition, J. Air Waste Manage., 58, 141–163, doi:10.3155/1047-3289.58.2.141, 2008.

DeCarlo, P. F., Kimmel, J. R., Trimborn, A., Northway, M. J., Jayne, J. T., Aiken, A. C., Gonin, M., Fuhrer, K., Horvath, T., Docherty, K. S., Worsnop, D. R., and Jimenez, J. L.: Field-Deployable, High-Resolution, Time-of-Flight Aerosol Mass Spectrometer, Anal. Chem., 78, 8281–8289, doi:10.1021/ac061249n, 2006.

Dillner, A. M. and Takahama, S.: Predicting ambient aerosol thermal-optical reflectance (TOR) measurements from infrared spectra: organic carbon, Atmos. Meas. Tech., 8, 1097–1109, doi:10.5194/amt-8-1097-2015, 2015.

Docherty, K. S., Aiken, A. C., Huffman, J. A., Ulbrich, I. M., DeCarlo, P. F., Sueper, D., Worsnop, D. R., Snyder, D. C., Peltier, R. E., Weber, R. J., Grover, B. D., Eatough, D. J., Williams, B. J., Goldstein, A. H., Ziemann, P. J., and Jimenez, J. L.: The 2005 Study of Organic Aerosols at Riverside (SOAR-1): instrumental intercomparisons and fine particle composition, Atmos. Chem. Phys., 11, 12387–12420, doi:10.5194/acp-11-12387-2011, 2011.

Drewnick, F., Schwab, J. J., Hogrefe, O., Peters, S., Husain, L., Diamond, D., Weber, R. and Demerjian, K. L.: Intercomparison and evaluation of four semi-continuous $PM_{2.5}$ sulfate instruments, Atmos. Environ., 37, 3335–3350, doi:10.1016/S1352-2310(03)00351-0, 2003.

Duarte, R. M. B. O., Freire, S. M. S. C., and Duarte, A. C.: Investigating the water-soluble organic functionality of urban aerosols using two-dimensional correlation of solid-state 13C NMR and FTIR spectral data, Atmos. Environ., 116, 245–252, doi:10.1016/j.atmosenv.2015.06.043, 2015.

Finessi, E., Decesari, S., Paglione, M., Giulianelli, L., Carbone, C., Gilardoni, S., Fuzzi, S., Saarikoski, S., Raatikainen, T., Hillamo, R., Allan, J., Mentel, Th. F., Tiitta, P., Laaksonen, A., Petäjä, T., Kulmala, M., Worsnop, D. R., and Facchini, M. C.: Determination of the biogenic secondary organic aerosol fraction in the boreal forest by NMR spectroscopy, Atmos. Chem. Phys., 12, 941–959, doi:10.5194/acp-12-941-2012, 2012.

Friedel, R. A., Shultz, J. L., and Sharkey, A. G.: Mass Spectrum of Nitric Acid, Anal. Chem., 31, 1128–1128, doi:10.1021/ac60150a615, 1959.

Fry, J. L., Draper, D. C., Zarzana, K. J., Campuzano-Jost, P., Day, D. A., Jimenez, J. L., Brown, S. S., Cohen, R. C., Kaser, L., Hansel, A., Cappellin, L., Karl, T., Hodzic Roux, A., Turnipseed, A., Cantrell, C., Lefer, B. L., and Grossberg, N.: Observations of gas- and aerosol-phase organic nitrates at BEACHON-RoMBAS 2011, Atmos. Chem. Phys., 13, 8585–8605, doi:10.5194/acp-13-8585-2013, 2013.

Gaffney, J. S., Marley, N. A., and Smith, K. J.: Characterization of Fine Mode Atmospheric Aerosols by Raman Microscopy and Diffuse Reflectance FTIR, J. Phys. Chem. A, 119, 4524–4532, doi:10.1021/jp510361s, 2015.

Goldstein, A. H. and Galbally, I. E.: Known and Unexplored Organic Constituents in the Earth's Atmosphere, Environ. Sci. Technol., 41, 1514–1521, 2007.

Goldstein, A. H., Worton, D. R., Williams, B. J., Hering, S. V., Kreisberg, N. M., Panić, O., and Górecki, T.: Thermal desorption comprehensive two-dimensional gas chromatography for in-situ measurements of organic aerosols, J. Chromatogr. A, 1186, 340–347, doi:10.1016/j.chroma.2007.09.094, 2008.

Graham, B.: Water-soluble organic compounds in biomass burning aerosols over Amazonia1. Characterization by NMR and GC-MS, J. Geophys. Res., 107, doi:10.1029/2001JD000336, 2002.

Hallquist, M., Wenger, J. C., Baltensperger, U., Rudich, Y., Simpson, D., Claeys, M., Dommen, J., Donahue, N. M., George, C., Goldstein, A. H., Hamilton, J. F., Herrmann, H., Hoffmann, T., Iinuma, Y., Jang, M., Jenkin, M. E., Jimenez, J. L., Kiendler-Scharr, A., Maenhaut, W., McFiggans, G., Mentel, Th. F., Monod, A., Prévôt, A. S. H., Seinfeld, J. H., Surratt, J. D., Szmigielski, R., and Wildt, J.: The formation, properties and impact of secondary organic aerosol: current and emerging issues, Atmos. Chem. Phys., 9, 5155–5236, doi:10.5194/acp-9-5155-2009, 2009.

Heald, C. L., Ridley, D. A., Kroll, J. H., Barrett, S. R. H., Cady-Pereira, K. E., Alvarado, M. J., and Holmes, C. D.: Contrasting the direct radiative effect and direct radiative forcing of aerosols, Atmos. Chem. Phys., 14, 5513–5527, doi:10.5194/acp-14-5513-2014, 2014.

Hering, S. and Cass, G.: The Magnitude of Bias in the Measurement of $PM_{2.5}$ Arising from Volatilization of Particulate Nitrate from Teflon Filters, J. Air Waste Manage., 49, 725–733, doi:10.1080/10473289.1999.10463843, 1999.

Holzinger, R., Williams, J., Herrmann, F., Lelieveld, J., Donahue, N. M., and Röckmann, T.: Aerosol analysis using a Thermal-Desorption Proton-Transfer-Reaction Mass Spectrometer (TD-PTR-MS): a new approach to study processing of organic aerosols, Atmos. Chem. Phys., 10, 2257–2267, doi:10.5194/acp-10-2257-2010, 2010.

Hu, W. W., Campuzano-Jost, P., Palm, B. B., Day, D. A., Ortega, A. M., Hayes, P. L., Krechmer, J. E., Chen, Q., Kuwata, M., Liu, Y. J., de Sá, S. S., McKinney, K., Martin, S. T., Hu, M., Budisulistiorini, S. H., Riva, M., Surratt, J. D., St. Clair, J. M., Isaacman-Van Wertz, G., Yee, L. D., Goldstein, A. H., Carbone, S., Brito, J., Artaxo, P., de Gouw, J. A., Koss, A., Wisthaler, A., Mikoviny, T., Karl, T., Kaser, L., Jud, W., Hansel, A., Docherty, K. S., Alexander, M. L., Robinson, N. H., Coe, H., Allan, J. D., Canagaratna, M. R., Paulot, F., and Jimenez, J. L.: Characterization of a real-time tracer for isoprene epoxydiols-derived secondary organic aerosol (IEPOX-SOA) from aerosol mass spectrometer measurements, Atmos. Chem. Phys., 15, 11807–11833, doi:10.5194/acp-15-11807-2015, 2015.

Huffman, J. A., Docherty, K. S., Aiken, A. C., Cubison, M. J., Ulbrich, I. M., DeCarlo, P. F., Sueper, D., Jayne, J. T., Worsnop, D. R., Ziemann, P. J., and Jimenez, J. L.: Chemically-resolved aerosol volatility measurements from two megacity field studies, Atmos. Chem. Phys., 9, 7161–7182, doi:10.5194/acp-9-7161-2009, 2009.

Isaacman, G., Kreisberg, N. M., Yee, L. D., Worton, D. R., Chan, A. W. H., Moss, J. A., Hering, S. V., and Goldstein, A. H.: Online derivatization for hourly measurements of gas- and particle-phase semi-volatile oxygenated organic compounds by thermal desorption aerosol gas chromatography (SV-TAG), Atmos. Meas. Tech., 7, 4417–4429, doi:10.5194/amt-7-4417-2014, 2014.

Jimenez, J. L., Canagaratna, M. R., Donahue, N. M., Prevot, A. S. H., Zhang, Q., Kroll, J. H., DeCarlo, P. F., Allan, J. D., Coe, H., Ng, N. L., Aiken, A. C., Docherty, K. S., Ulbrich, I. M., Grieshop, A. P., Robinson, A. L., Duplissy, J., Smith, J. D., Wilson, K. R., Lanz, V. A., Hueglin, C., Sun, Y. L., Tian, J., Laaksonen, A., Raatikainen, T., Rautiainen, J., Vaattovaara, P., Ehn, M., Kulmala, M., Tomlinson, J. M., Collins, D. R., Cubison, M. J., E., Dunlea, J., Huffman, J. A., Onasch, T. B., Alfarra, M. R., Williams, P. I., Bower, K., Kondo, Y., Schneider, J., Drewnick, F., Borrmann, S., Weimer, S., Demerjian, K., Salcedo, D., Cottrell, L., Griffin, R., Takami, A., Miyoshi, T., Hatakeyama, S., Shimono, A., Sun, J. Y., Zhang, Y. M., Dzepina, K., Kimmel, J. R., Sueper, D., Jayne, J. T., Herndon, S. C., Trimborn, A. M., Williams, L. R., Wood, E. C., Middlebrook, A. M., Kolb, C. E., Baltensperger, U., and Worsnop, D. R.: Evolution of Organic Aerosols in the Atmosphere, Science, 326, 1525–1529, doi:10.1126/science.1180353, 2009.

Kim, E., Hopke, P. K., Pinto, J. P. and Wilson, W. E.: Spatial Variability of Fine Particle Mass, Components, and Source Contributions during the Regional Air Pollution Study in St. Louis, Environ. Sci. Technol., 39, 4172–4179, doi:10.1021/es049824x, 2005.

Kreisberg, N. M., Hering, S. V., Williams, B. J., Worton, D. R. and Goldstein, A. H.: Quantification of Hourly Speciated Organic Compounds in Atmospheric Aerosols, Measured by an In-Situ Thermal Desorption Aerosol Gas Chromatograph (TAG), Aerosol Sci. Tech., 43, 38–52, doi:10.1080/02786820802459583, 2009.

Kroll, J. H., Donahue, N. M., Jimenez, J. L., Kessler, S. H., Canagaratna, M. R., Wilson, K. R., Altieri, K. E., Mazzoleni, L. R., Wozniak, A. S., Bluhm, H., Mysak, E. R., Smith, J. D., Kolb, C. E., and Worsnop, D. R.: Carbon oxidation state as a metric for describing the chemistry of atmospheric organic aerosol, Nat. Chem., 3, 133–139, doi:10.1038/nchem.948, 2011.

Lambe, A., Chacon-Madrid, H., Nguyen, N., Weitkamp, E., Kreisberg, N., Hering, S., Goldstein, A., Donahue, N. and Robinson, A.: Organic Aerosol Speciation: Intercomparison of Thermal Desorption Aerosol GC/MS (TAG) and Filter-Based Techniques, Aerosol Sci. Tech., 44, 141–151, 2010.

Lambe, A. T., Logue, J. M., Kreisberg, N. M., Hering, S. V., Worton, D. R., Goldstein, A. H., Donahue, N. M., and Robinson, A. L.: Apportioning black carbon to sources using highly time-resolved ambient measurements of organic molecular markers in Pittsburgh, Atmos. Environ., 43, 3941–3950, 2009.

Lanz, V. A., Alfarra, M. R., Baltensperger, U., Buchmann, B., Hueglin, C., and Prévôt, A. S. H.: Source apportionment of submicron organic aerosols at an urban site by factor analytical modelling of aerosol mass spectra, Atmos. Chem. Phys., 7, 1503–1522, doi:10.5194/acp-7-1503-2007, 2007.

Lim, Y. B. and Ziemann, P. J.: Chemistry of Secondary Organic Aerosol Formation from OH Radical-Initiated Reactions of Linear, Branched, and Cyclic Alkanes in the Presence of NO_x, Aerosol Sci. Tech., 43, 604–619, doi:10.1080/02786820902802567, 2009.

Lin, Y.-H., Zhang, Z., Docherty, K. S., Zhang, H., Budisulistiorini, S. H., Rubitschun, C. L., Shaw, S. L., Knipping, E. M., Edgerton, E. S., Kleindienst, T. E., Gold, A., and Surratt, J. D.: Isoprene Epoxydiols as Precursors to Secondary Organic Aerosol Formation: Acid-Catalyzed Reactive Uptake Studies with Authentic Compounds, Environ. Sci. Technol., 46, 250–258, doi:10.1021/es202554c, 2012.

Lopez-Hilfiker, F. D., Mohr, C., Ehn, M., Rubach, F., Kleist, E., Wildt, J., Mentel, Th. F., Lutz, A., Hallquist, M., Worsnop, D., and Thornton, J. A.: A novel method for online analysis of gas and particle composition: description and evaluation of a Filter Inlet for Gases and AEROsols (FIGAERO), Atmos. Meas. Tech., 7, 983–1001, doi:10.5194/amt-7-983-2014, 2014.

Martinez, R., Williams, B. J., Zhang, Y., Hagan, D., Walker, M., Kreisberg, N. M., Hering, S. V., Hohaus, T., Jayne, J. T., and Worsnop, D. R.: Development of a Volatility and Polarity Separator (VAPS) for Volatility- and Polarity-Resolved Organic Aerosol Measurement, Aerosol Sci. Tech., accepted, 2015.

Mauderly, J. L. and Chow, J. C.: Health Effects of Organic Aerosols, Inhal. Toxicol., 20, 257–288, doi:10.1080/08958370701866008, 2008.

Meyer, M. B., Patashnick, H., Ambs, J. L., and Rupprecht, E.: Development of a Sample Equilibration System for the TEOM Continuous PM Monitor, J. Air Waste Manage., 50, 1345–1349, doi:10.1080/10473289.2000.10464180, 2000.

Middlebrook, A. M., Bahreini, R., Jimenez, J. L., and Canagaratna, M. R.: Evaluation of Composition-Dependent Collection Efficiencies for the Aerodyne Aerosol Mass Spectrometer using Field Data, Aerosol Sci. Tech., 46, 258–271, doi:10.1080/02786826.2011.620041, 2012.

Nejedlý, Z., Campbell, J. L., Teesdale, W. J., Dlouhy, J. F., Dann, T. F., Hoff, R. M., Brook, J. R., and Wiebe, H. A.: Inter-Laboratory Comparison of Air Particulate Monitoring Data, J. Air Waste Manage., 48, 386–397, doi:10.1080/10473289.1998.10463698, 1998.

Ng, N. L., Canagaratna, M. R., Zhang, Q., Jimenez, J. L., Tian, J., Ulbrich, I. M., Kroll, J. H., Docherty, K. S., Chhabra, P. S., Bahreini, R., Murphy, S. M., Seinfeld, J. H., Hildebrandt, L., Donahue, N. M., DeCarlo, P. F., Lanz, V. A., Prévôt, A. S. H., Dinar, E., Rudich, Y., and Worsnop, D. R.: Organic aerosol components observed in Northern Hemispheric datasets from Aerosol Mass Spectrometry, Atmos. Chem. Phys., 10, 4625–4641, doi:10.5194/acp-10-4625-2010, 2010.

Ng, N. L., Herndon, S. C., Trimborn, A., Canagaratna, M. R., Croteau, P. L., Onasch, T. B., Sueper, D., Worsnop, D. R., Zhang, Q., Sun, Y. L., and Jayne, J. T.: An Aerosol Chemical Speciation Monitor (ACSM) for Routine Monitoring of the Composition and Mass Concentrations of Ambient Aerosol, Aerosol Sci. Tech., 45, 780–794, doi:10.1080/02786826.2011.560211, 2011.

Nozière, B., Kalberer, M., Claeys, M., Allan, J., D'Anna, B., Decesari, S., Finessi, E., Glasius, M., Grgić, I., Hamilton, J. F., Hoffmann, T., Iinuma, Y., Jaoui, M., Kahnt, A., Kampf, C. J., Kourtchev, I., Maenhaut, W., Marsden, N., Saarikoski, S., Schnelle-Kreis, J., Surratt, J. D., Szidat, S., Szmigielski, R., and Wisthaler, A.: The Molecular Identification of Organic Compounds in the Atmosphere: State of the Art and Challenges, Chem. Rev., 115, 3919–3983, doi:10.1021/cr5003485, 2015.

Pope, C. A. and Dockery, D. W.: Health Effects of Fine Particulate Air Pollution: Lines that Connect, J. Air Waste Manage., 56, 709–742, doi:10.1080/10473289.2006.10464485, 2006.

Robinson, N. H., Hamilton, J. F., Allan, J. D., Langford, B., Oram, D. E., Chen, Q., Docherty, K., Farmer, D. K., Jimenez, J. L., Ward, M. W., Hewitt, C. N., Barley, M. H., Jenkin, M. E., Rickard, A. R., Martin, S. T., McFiggans, G., and Coe, H.: Evidence for a significant proportion of Secondary Organic Aerosol from isoprene above a maritime tropical forest, Atmos. Chem. Phys., 11, 1039–1050, doi:10.5194/acp-11-1039-2011, 2011.

Schlesinger, R. B., Kunzli, N., Hidy, G. M., Gotschi, T., and Jerrett, M.: The Health Relevance of Ambient Particulate Matter Characteristics: Coherence of Toxicological and Epidemiological Inferences, Inhal. Toxicol., 18, 95–125, doi:10.1080/08958370500306016, 2006.

Slowik, J. G., Brook, J., Chang, R. Y.-W., Evans, G. J., Hayden, K., Jeong, C.-H., Li, S.-M., Liggio, J., Liu, P. S. K., McGuire, M., Mihele, C., Sjostedt, S., Vlasenko, A., and Abbatt, J. P. D.: Photochemical processing of organic aerosol at nearby continental sites: contrast between urban plumes and regional aerosol, Atmos. Chem. Phys., 11, 2991–3006, doi:10.5194/acp-11-2991-2011, 2011.

Stolzenburg, M. R. and Hering, S. V.: Method for the Automated Measurement of Fine Particle Nitrate in the Atmosphere, Environ. Sci. Technol., 34, 907–914, doi:10.1021/es990956d, 2000.

Tobias, H. J., Kooiman, P. M., Docherty, K. S., and Ziemann, P. J.: Real-Time Chemical Analysis of Organic Aerosols Using a Thermal Desorption Particle Beam Mass Spectrometer, Aerosol Sci. Tech., 33, 170–190, doi:10.1080/027868200410912, 2000.

Tobias, H. J., Beving, D. E., Ziemann, P. J., Sakurai, H., Zuk, M., McMurry, P. H., Zarling, D., Waytulonis, R., and Kittelson, D. B.: Chemical Analysis of Diesel Engine Nanoparticles Using a Nano-DMA/Thermal Desorption Particle Beam Mass Spectrometer, Environ. Sci. Technol., 35, 2233–2243, doi:10.1021/es0016654, 2001.

Ulbrich, I. M., Canagaratna, M. R., Zhang, Q., Worsnop, D. R., and Jimenez, J. L.: Interpretation of organic components from Positive Matrix Factorization of aerosol mass spectrometric data, Atmos. Chem. Phys., 9, 2891–2918, doi:10.5194/acp-9-2891-2009, 2009.

Wang, Y., Khalizov, A., Levy, M., and Zhang, R.: New Directions: Light absorbing aerosols and their atmospheric impacts, Atmos. Environ., 81, 713–715, doi:10.1016/j.atmosenv.2013.09.034, 2013.

Weber, R.: Intercomparison of near real time monitors of $PM_{2.5}$ nitrate and sulfate at the U.S. Environmental Protection Agency Atlanta Supersite, J. Geophys. Res., 108, 8421, doi:10.1029/2001JD001220, 2003.

Weber, R. J., Orsini, D., Duan, Y., Lee, Y.-N., Klotz, P. J., and Brechtel, F.: A particle-into-liquid collector for rapid measurement of aerosol bulk chemical composition, Aerosol Sci. Tech., 35, 718–727, 2001.

Williams, B. J., Goldstein, A. H., Kreisberg, N. M., and Hering, S. V.: An In-Situ Instrument for Speciated Organic Composition of Atmospheric Aerosols: Thermal Desorption Aerosol GC/MS-FID (TAG), Aerosol Sci. Tech., 40, 627–638, doi:10.1080/02786820600754631, 2006.

Williams, B. J., Goldstein, A. H., Millet, D. B., Holzinger, R., Kreisberg, N. M., Hering, S. V., White, A. B., Worsnop, D. R., Allan, J. D., and Jimenez, J. L.: Chemical speciation of organic aerosol during the International Consortium for Atmospheric Research on Transport and Transformation 2004: Results from in situ measurements, J. Geophys. Res., 112, D10S26, doi:10.1029/2006JD007601, 2007.

Williams, B. J., Goldstein, A. H., Kreisberg, N. M., Hering, S. V., Worsnop, D. R., Ulbrich, I. M., Docherty, K. S., and Jimenez, J. L.: Major components of atmospheric organic aerosol in southern California as determined by hourly measurements of source marker compounds, Atmos. Chem. Phys., 10, 11577–11603, doi:10.5194/acp-10-11577-2010, 2010.

Williams, B. J., Jayne, J. T., Lambe, A. T., Hohaus, T., Kimmel, J. R., Sueper, D., Brooks, W., Williams, L. R., Trimborn, A. M., Martinez, R. E., Hayes, P. L., Jimenez, J. L., Kreisberg, N. M., Hering, S. V., Worton, D. R., Goldstein, A. H., and Worsnop, D. R.: The First Combined Thermal Desorption Aerosol Gas Chromatograph–Aerosol Mass Spectrometer (TAG-AMS), Aerosol Sci. Tech., 48, 358–370, doi:10.1080/02786826.2013.875114, 2014.

Worton, D. R., Goldstein, A. H., Farmer, D. K., Docherty, K. S., Jimenez, J. L., Gilman, J. B., Kuster, W. C., de Gouw, J., Williams, B. J., Kreisberg, N. M., Hering, S. V., Bench, G., McKay, M., Kristensen, K., Glasius, M., Surratt, J. D., and Seinfeld, J. H.: Origins and composition of fine atmospheric carbonaceous aerosol in the Sierra Nevada Mountains, California, Atmos. Chem. Phys., 11, 10219–10241, doi:10.5194/acp-11-10219-2011, 2011.

Yamamoto, M. and Kosaka, H.: Determination of nitrate in deposited aerosol particles by thermal decomposition and chemiluminescence, Anal. Chem., 66, 362–367, doi:10.1021/ac00075a009, 1994.

Yatavelli, R. L. N., Lopez-Hilfiker, F., Wargo, J. D., Kimmel, J. R., Cubison, M. J., Bertram, T. H., Jimenez, J. L., Gonin, M., Worsnop, D. R., and Thornton, J. A.: A Chemical Ionization High-Resolution Time-of-Flight Mass Spectrometer Coupled to a Micro Orifice Volatilization Impactor (MOVI-HRToF-CIMS) for Analysis of Gas and Particle-Phase Organic Species, Aerosol Sci. Tech., 46, 1313–1327, doi:10.1080/02786826.2012.712236, 2012.

Yu, J. Z., Huang, X. H. H., Ho, S. S. H., and Bian, Q.: Nonpolar organic compounds in fine particles: quantification by thermal desorption–GC/MS and evidence for their significant oxidation in ambient aerosols in Hong Kong, Anal. Bioanal. Chem., 401, 3125–3139, doi:10.1007/s00216-011-5458-5, 2011.

Yu, X.-Y., Lee, T., Ayres, B., Kreidenweis, S. M., Collett, J. L., and Malm, W.: Particulate Nitrate Measurement Using Nylon Filters, J. Air Waste Manage., 55, 1100–1110, doi:10.1080/10473289.2005.10464721, 2005.

Zhang, Y., Williams, B. J., Goldstein, A. H., Docherty, K., Ulbrich, I. M., and Jimenez, J. L.: A Technique for Rapid Gas Chromatography Analysis Applied to Ambient Organic Aerosol Measurements from the Thermal Desorption Aerosol Gas Chromatograph (TAG), Aerosol Sci. Tech., 48, 1166–1182, doi:10.1080/02786826.2014.967832, 2014.

Zhao, Y., Kreisberg, N. M., Worton, D. R., Teng, A. P., Hering, S. V., and Goldstein, A. H.: Development of an *In Situ* Thermal Desorption Gas Chromatography Instrument for Quantifying Atmospheric Semi-Volatile Organic Compounds, Aerosol Sci. Tech., 47, 258–266, doi:10.1080/02786826.2012.747673, 2013.

Table 1. Correlations (Pearson r) between AMS components and TAG components during two field studies (SOAR 2005 and SLAQRS 2013).

	SOAR – Riverside, CA 2005			SLAQRS – East St. Louis, IL 2013		
AMS data	TAG decomp. m/z 43 (particle)	TAG decomp. m/z 44 (particle)	TAG main chromatogram (total ion signal – background column)	TAG decomp. m/z 43 (particle)	TAG decomp. m/z 44 (particle)	TAG main chromatogram (total ion signal – background column)
Organics	0.21	0.51	0.56	0.67	0.46	0.61
$m/z43$	0.49	0.56	0.52	0.54	0.40	0.71
$m/z44$	0.49	0.70	0.29	0.50	0.41	0.28
$C_2H_3O^+$	0.46	0.61	0.32	0.67	0.54	0.47
CO_2^+	0.48	0.70	0.29	0.50	0.35	0.15
HOA	−0.06	0.02	0.60	0.03	−0.08	0.60
OOA	0.58	0.55	0.36	0.82	0.58	0.32
cLV-OOA	0.26	0.73	0.26	PMF not complete for higher factor solution		
(subcomponent of LV-OOA)	0.60	0.90	0.20			
MV-OOA	0.29	0.50	0.42			
SV-OOA	−0.32	−0.47	−0.07			
LOA-AC	−0.07	0.23	−0.02			
LOA2	−0.17	−0.07	−0.30			
HOA + MVOOA	0.24	0.42	0.76			
HOA + MVOOA + SVOOA	0.11	0.22	0.72			
HOA + MVOOA + cLVOOA	0.27	0.61	0.59			
All PMF – cLVOOA	0.07	0.24	0.68			

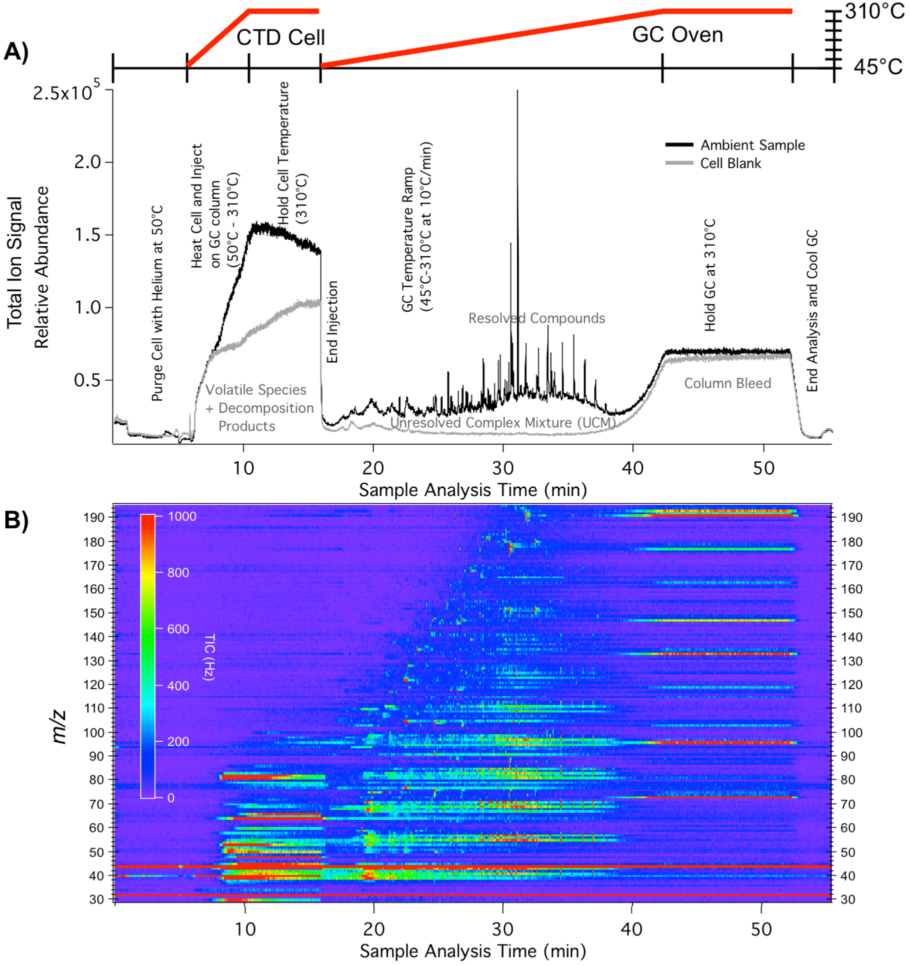

A)
CTD Cell
GC Oven
310°C
45°C
2.5x10^5
2.0
1.5
1.0
0.5
Total Ion Signal
Relative Abundance
Purge Cell with Helium at 50°C
Heat Cell and Inject on GC column (50°C - 310°C)
Hold Cell Temperature (310°C)
End Injection
GC Temperature Ramp (45°C-310°C at 10°C/min)
Hold GC at 310°C
End Analysis and Cool GC
Ambient Sample
Cell Blank
Volatile Species + Decomposition Products
Resolved Compounds
Unresolved Complex Mixture (UCM)
Column Bleed
10
20
30
40
50
Sample Analysis Time (min)
B)
m/z
190
180
170
160
150
140
130
120
110
100
90
80
70
60
50
40
30
1000
800
600
400
200
0
TIC (Hz)
10
20
30
40
50
Sample Analysis Time (min)

Figure 1. Example TAG sample from SLAQRS 2013 in East St. Louis, IL. **(a)** Total ion signal on the MS detector (y axis) plotted as a function of sample analysis time in minutes (x axis). The black trace is from an ambient sample, compared to a cell blank (thermal cycling with no aerosol collection) plotted in gray. Red curves above the figure display temperature profiles for the TAG CTD Cell during sample injection, and then the GC oven during molecular analysis. The TAG CTD Cell purges water/solvent then heats and delivers sample onto the GC column during the sample analysis time < 17 min. It is here that thermal decomposition products travel through the GC column (which is at a cooler 45 °C) and directly to the detector. Traditional GC operation will not collect data during this period, using a solvent delay, to prevent detector degradation. **(b)** 3-D plot of the same ambient sample from Fig. 1a, but now displaying the additional information stored in the mass spectra obtained several times every second. Here it is seen that almost all of the thermal decomposition analysis window signal is produced by ions $< m/z$ 100.

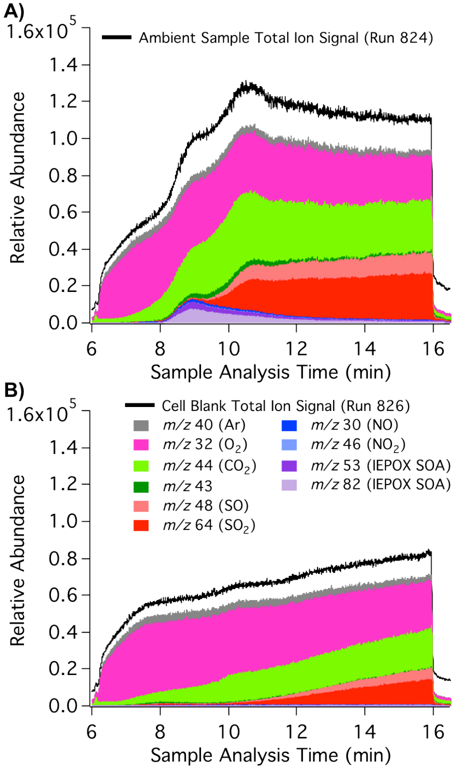

Figure 2. Example **(a)** ambient, and **(b)** cell blank samples as analyzed by the TAG instrument. Shown here is the sample injection time period where the TAG CTD cell is heated and delivers material from the particle collector to the GC column. Any signal present in this time window is from volatile molecules or thermal decomposition products that can elute through a 30 m GC column held at a cool temperature of 45 °C.

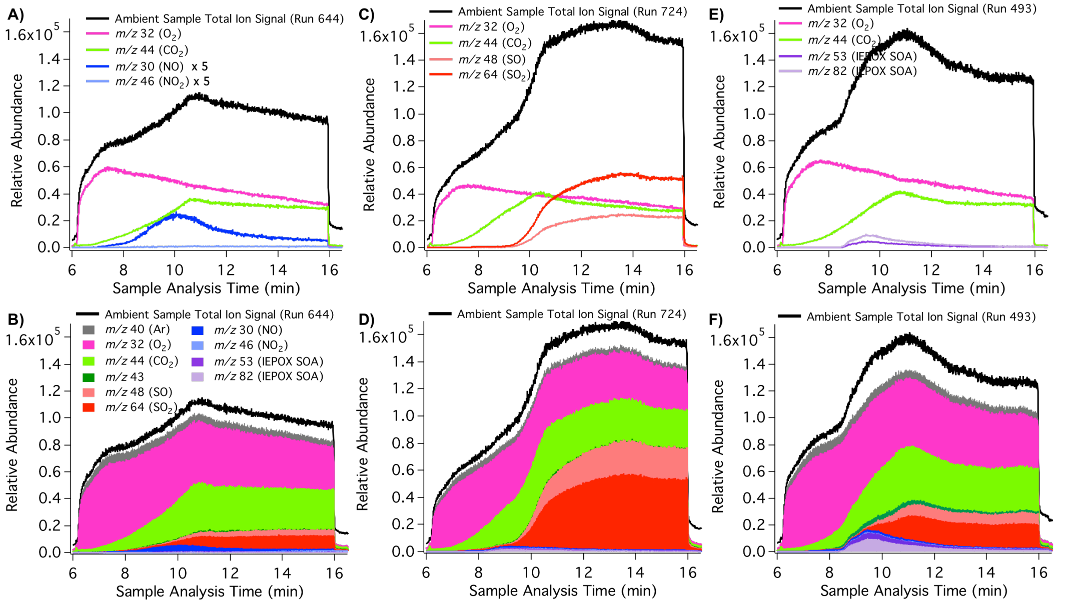

Figure 3. Thermal decomposition product window observed by the TAG system for three different aerosol types observed during the SLAQRS field campaign. Panels **(a–b)** show a sample that had a relatively elevated m/z 30 signal (both m/z 30 and 46 are increased by a factor of 5 in panel **(a)** to help display trend vs. sample analysis time), panels **(c–d)** show a sample that had relatively elevated m/z 48 and m/z 64, and panels **(e–f)** show a sample that had relatively elevated m/z 53 and m/z 82. The top panels of each set **(a, c, e)** display individual ions of interest, and the bottom panels **(b, d, f)** show cumulative traces of all major ions.

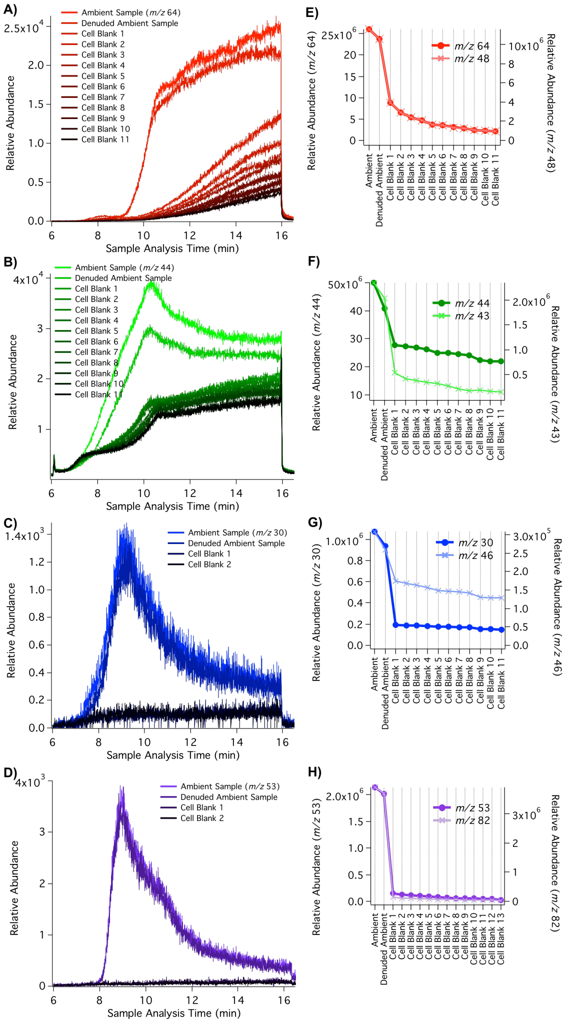
A)
2.5x10^4
2.0
1.5
1.0
0.5
0.0
Relative Abundance
6 8 10 12 14 16
Sample Analysis Time (min)
Ambient Sample (m/z 64)
Denuded Ambient Sample
Cell Blank 1
Cell Blank 2
Cell Blank 3
Cell Blank 4
Cell Blank 5
Cell Blank 6
Cell Blank 7
Cell Blank 8
Cell Blank 9
Cell Blank 10
Cell Blank 11
E)
25x10^6
20
15
10
5
0
Relative Abundance (m/z 64)
10x10^6
8
6
4
2
0
Relative Abundance (m/z 48)
m/z 64
m/z 48
Ambient
Denuded Ambient
Cell Blank 1
Cell Blank 2
Cell Blank 3
Cell Blank 4
Cell Blank 5
Cell Blank 6
Cell Blank 7
Cell Blank 8
Cell Blank 9
Cell Blank 10
Cell Blank 11
B)
4x10^4
3
2
1
Relative Abundance
6 8 10 12 14 16
Sample Analysis Time (min)
Ambient Sample (m/z 44)
Denuded Ambient Sample
Cell Blank 1
Cell Blank 2
Cell Blank 3
Cell Blank 4
Cell Blank 5
Cell Blank 6
Cell Blank 7
Cell Blank 8
Cell Blank 9
Cell Blank 10
Cell Blank 11
F)
50x10^6
40
30
20
10
Relative Abundance (m/z 44)
2.0x10^6
1.5
1.0
0.5
Relative Abundance (m/z 43)
m/z 44
m/z 43
Ambient
Denuded Ambient
Cell Blank 1
Cell Blank 2
Cell Blank 3
Cell Blank 4
Cell Blank 5
Cell Blank 6
Cell Blank 7
Cell Blank 8
Cell Blank 9
Cell Blank 10
Cell Blank 11
C)
1.4x10^3
1.2
1.0
0.8
0.6
0.4
0.2
0.0
Relative Abundance
6 8 10 12 14 16
Sample Analysis Time (min)
Ambient Sample (m/z 30)
Denuded Ambient Sample
Cell Blank 1
Cell Blank 2
G)
1.0x10^6
0.8
0.6
0.4
0.2
0.0
Relative Abundance (m/z 30)
3.0x10^5
2.5
2.0
1.5
1.0
0.5
0.0
Relative Abundance (m/z 46)
m/z 30
m/z 46
Ambient
Denuded Ambient
Cell Blank 1
Cell Blank 2
Cell Blank 3
Cell Blank 4
Cell Blank 5
Cell Blank 6
Cell Blank 7
Cell Blank 8
Cell Blank 9
Cell Blank 10
Cell Blank 11
D)
4x10^3
3
2
1
0
Relative Abundance
6 8 10 12 14 16
Sample Analysis Time (min)
Ambient Sample (m/z 53)
Denuded Ambient Sample
Cell Blank 1
Cell Blank 2
H)
2.0x10^6
1.5
1.0
0.5
0.0
Relative Abundance (m/z 53)
3x10^6
2
1
0
Relative Abundance (m/z 82)
m/z 53
m/z 82
Ambient
Denuded Ambient
Cell Blank 1
Cell Blank 2
Cell Blank 3
Cell Blank 4
Cell Blank 5
Cell Blank 6
Cell Blank 7
Cell Blank 8
Cell Blank 9
Cell Blank 10
Cell Blank 11
Cell Blank 12
Cell Blank 13

Figure 4. Exploration of sample carryover in the thermal decomposition window between samples for a **(a)** sulfate tracer ion (m/z 64), **(b)** organics tracer ion (m/z 44), **(c)** nitrate tracer ion (m/z 30), and **(d)** isoprene-derived SOA tracer ion (m/z 53). All panels show consecutive ambient sample (particle+gas fractions), denuded sample (particle-only), followed by repeated cell blanks (sample valves open, but no sample is pulled through collector). Panels **(e–h)** display quantified signals for associated ions across the decomposition window (6–16 min). The sulfate tracers (m/z 48, 64) and organics tracers (m/z 43, 44) show measurable carryover during the first couple cell blanks. All tracer ions have some elevated background that remains after repeat cell blanks, but the organics tracer m/z 44 and nitrate tracer m/z 46 have the largest background signal.

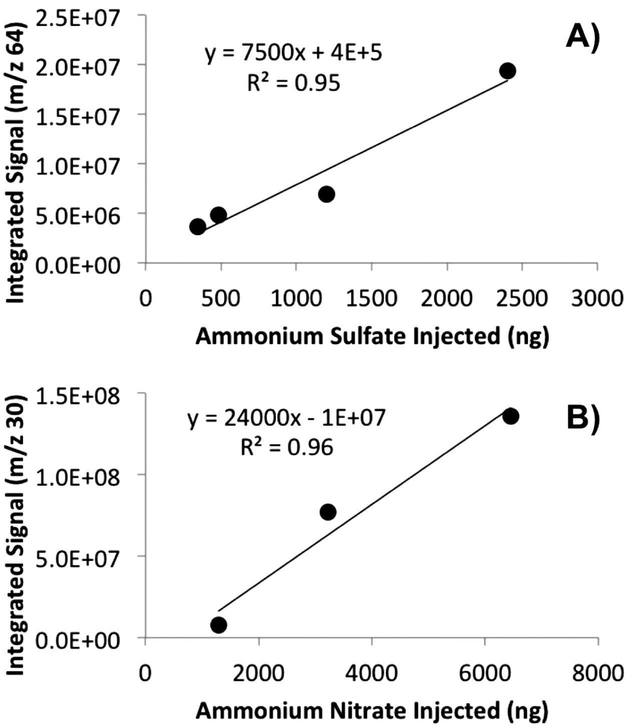

Figure 5. Inorganic calibration standards introduced to the TAG CTD cell through syringe injection. Major decomposition ions were integrated across the decomposition window (6–16 min) and are plotted with injected mass of **(a)** ammonium sulfate (tracked by m/z 64), and **(b)** ammonium nitrate (tracked by m/z 30).

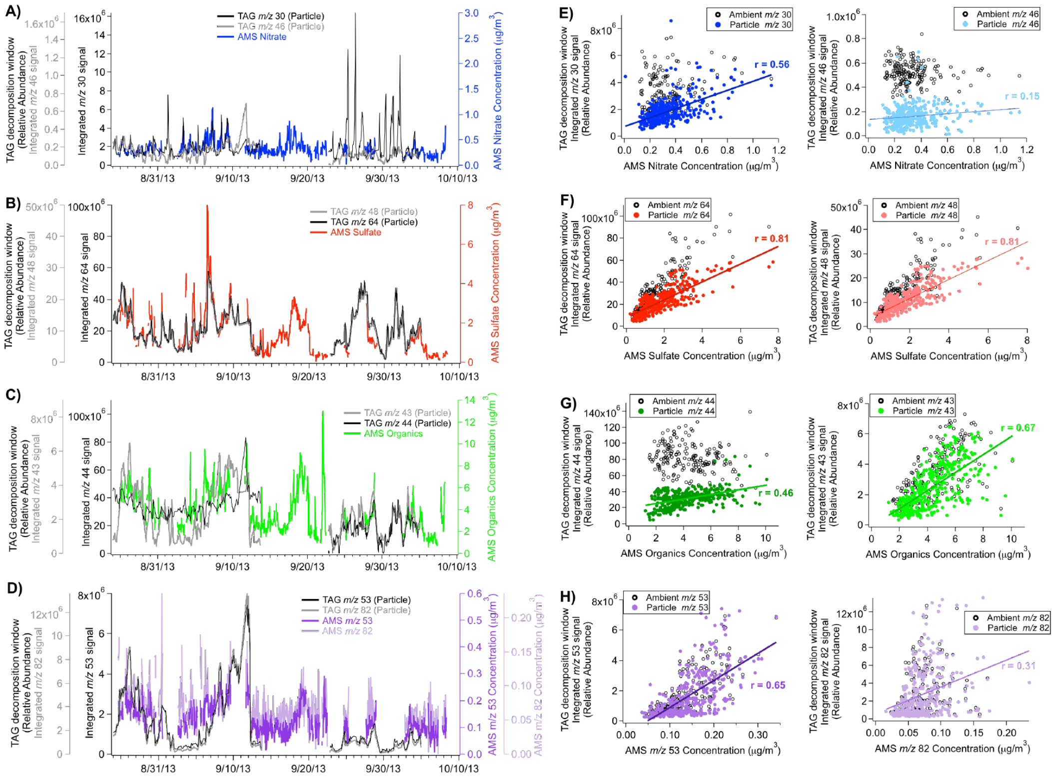

Figure 6. Timeseries and correlations of TAG decomposition fragments and corresponding AMS chemical species during SLAQRS 2013 in East St. Louis, IL. Panels **(a–d)** show timeseries of AMS nitrate, organics, sulfate, and m/z 53 (tracer for isoprene-derived SOA) plotted with TAG decomposition ions m/z 30, 44, 64, 53, respectively. It can be observed in panels **(e–h)** that good correlations are observed between TAG decomposition fragments and AMS species after determining a particle-only signal (background and gas-phase signal subtracted) for the TAG tracers.

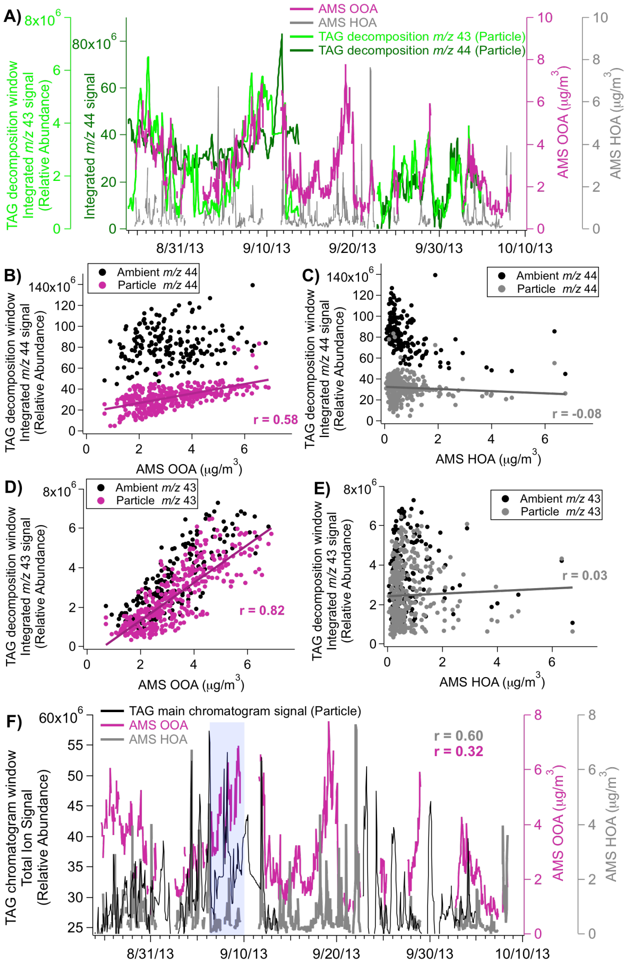

Title Page
Abstract | Introduction
Conclusions | References
Tables | Figures
◀| |▶
◀ ▶
Back | Close
Full Screen / Esc
Printer-friendly Version
Interactive Discussion

Figure 7. Comparisons of particle-only TAG components and corresponding AMS two factor PMF components, oxygenated organic aerosol (OOA) and hydrocarbon-like OA (HOA) during SLAQRS 2013 in East St. Louis, IL. **(a)** Timeseries of particle-only TAG decomposition m/z 43 and 44 signal and AMS PMF components (OOA, HOA). **(b)** A higher correlation ($r = 0.58$) is observed between TAG decomposition m/z 44 and AMS OOA than between **(c)** TAG decomposition m/z 44 and AMS HOA ($r = -0.08$). **(d)** A higher correlation ($r = 0.82$) is observed between TAG decomposition m/z 43 and AMS OOA than between **(e)** TAG decomposition m/z 43 and AMS HOA ($r = 0.03$). **(f)** Integrating the TAG total ion signal within the traditional chromatogram time window (16–45 min) and subtracting contributions from column background and gas-phase fraction, yields a higher correlation with AMS HOA ($r = 0.60$) than with AMS OOA ($r = 0.32$). The correlations are even more extreme ($r = 0.76$ with HOA, and $r = 0.18$ with OOA) if the short time period of high isoprene SOA impact between 6–10 September 2013 (highlighted in light blue) is removed.

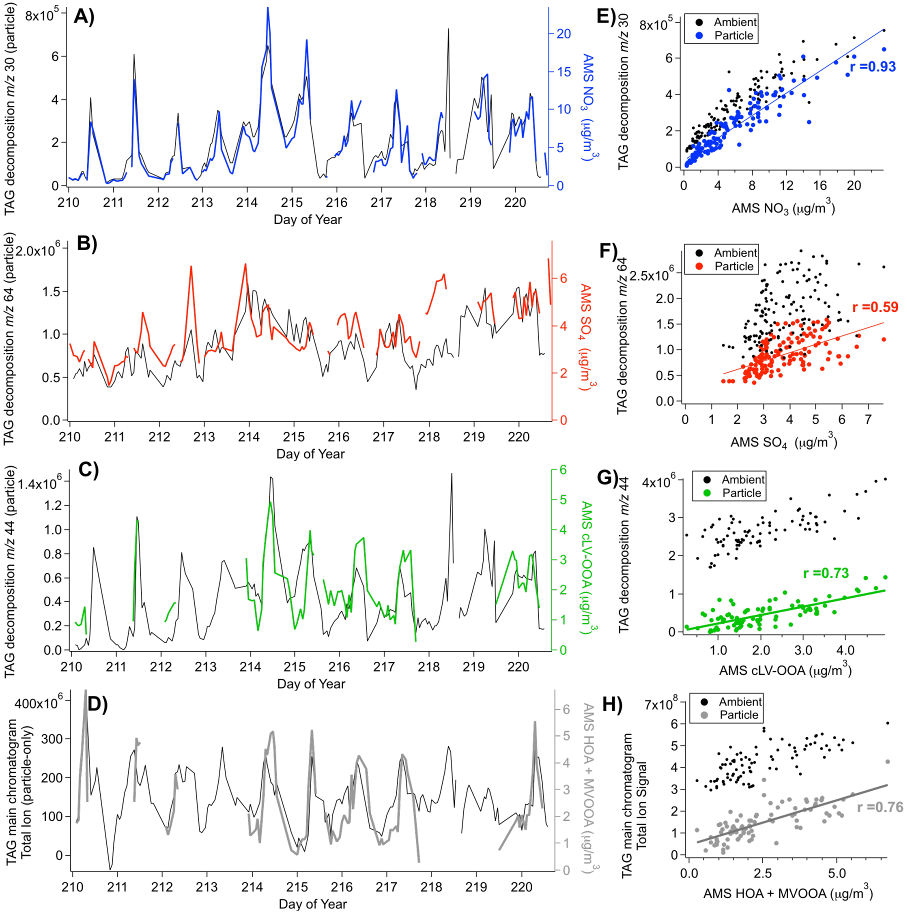

Figure 8. Correlations between TAG decomposition fragments and AMS species during SOAR 2005 in Riverside, CA.

Title Page
Abstract | Introduction
Conclusions | References
Tables | Figures
◀| |▶
◀ ▶
Back | Close
Full Screen / Esc
Printer-friendly Version
Interactive Discussion